# Modeling molecular interactions to understand spatial crowding effects on heterodimer formations

K. M. Puskar,[1] A. Parisi-Amon,[2] S. Ta'asan,[3] R. Schwartz,[4] and P. R. LeDuc[5,4]
[1]*MechanoBiology Laboratory, Department of Orthopaedic Surgery, University of Pittsburgh, Pennsylvania 15213, USA*
[2]*Department of Biomedical Engineering, Duke University, Durham, North Carolina 27701, USA*
[3]*Mathematical Science, Carnegie Mellon University, Pittsburgh, Pennsylvania 15122, USA*
[4]*Biological and Computer Science, Carnegie Mellon University, Pittsburgh, Pennsylvania 15122, USA*
[5]*Department of Mechanical Engineering, Carnegie Mellon University, Pittsburgh, Pennsylvania 15122, USA*
(Received 4 May 2007; published 8 October 2007)

Molecular crowding occurs when the density of interacting molecules in some reaction system is sufficient to create deviations from traditional mass-action models of chemistry in diffusive systems. While there is a great deal of theory on the influence of molecular crowding on biochemistry *in vivo*, the effects are highly dependent on specific assumptions about the shapes, volumes, and diffusion properties of the components of an individual system and are thus difficult to predict from first principles. In this study, we use lattice Monte Carlo simulations to examine the effects on a reaction system for two limiting cases of the diffusion behavior of inert crowding agents. In cells, inert molecules might diffuse throughout a solute along with the reactant species by passive diffusion or may be anchored at fixed positions within the solute. We investigate the relative contributions of the two models to crowding effects by examining moving inert particles versus stationery inert particles on the kinetics of a heterodimer assembly system. The two models of inert crowding agents resulted in highly divergent effects on the reactant system. Stationary particles exhibited a bimodal response in the reaction rate curve that was a function of copy number and spatial arrangement and which accelerated the process at conditions not unlike those found in cellular environments. On the other hand, moving inert particles created a well mixed background that had no effect on the reaction process even under extremely compacted conditions. These results may have applications in developing more realistic simulations of reaction chemistry in crowded environments such as living cells.

DOI: 10.1103/PhysRevE.76.041904 PACS number(s): 87.15.Aa, 05.10.Ln, 82.39.Rt

## INTRODUCTION

Cell environments are known to be complex, heterogeneous distributions of multitudes of chemical species. Computer models of these systems must necessarily make many simplifying assumptions, typically carried over from well-established models of solution chemistry. These commonly include the implicit assumptions that reaction systems act in a dilute, well mixed media consisting of only the reactants to the particular reaction under study. The standard model for such systems is a system of ordinary differential equations derived from the law of mass action, which assumes an environment that is homogenous, continuous, and deterministic. Reactions *in vivo*, however, typically occur under conditions in which other background molecules and stationary structures occur within a complex, highly constrained geometry [1]. The reactions are the result of discrete collisions between finite populations of molecules through passive diffusion or a finely orchestrated transport system, and therefore have an inherently stochastic component. There are now many examples of reaction systems in which this stochastic behavior appears to be essential to biological function [28,2,3].

The true cellular environment is densely packed with a variety of macromolecules, on the order of 50–400 mg/ml, suggesting that 10%–40% of the total cell volume is occupied by these molecules [5–8]. Though these surrounding molecules and structures are not formally considered reactants for most of the chemistry occurring in the cell, they can nonetheless have sizable effects on the thermodynamics and kinetics of a broad range of reactions occurring in the cell [9,1,10]. This phenomenon is referred to as crowding. Crowding is believed to exert a nonspecific effect on reaction processes primarily through two mechanisms. It reduces the reaction space available to the reacting species, producing an entropic effect called the excluded volume effect that tends to enhance binding events. Conversely, it impedes molecular diffusion, which can reduce the rate at which the reactants meet. These opposing effects can alter reaction rates and equilibria as compared with a dilute well mixed media [11]. Where a process is diffusion limited, crowding will tend to reduce the association rate and impede the reaction. Reactions limited by transition times for changes in state are likely to be promoted. An example of the latter process is provided by recent molecular dynamics studies of the binding of Cdc42 to CBD, where a significant amount of folding appears to be necessary after initial binding to generate a fully bound dimer [12]. Most biological processes occurring *in vivo* are influenced by both effects to some degree and either may dominate a given reaction system depending on the nature and concentration of the crowding agent. In the extreme the binding rate is dominated by the encounter rate and at high enough concentrations will fall even for transition state limited reactions.

Experiments [13–16] and theoretical models [17–21] indicate that the dominating effect of crowding on a reaction process depends strongly on the size, shape, and arrangement of the surrounding obstacles. It is more pronounced for larger

 

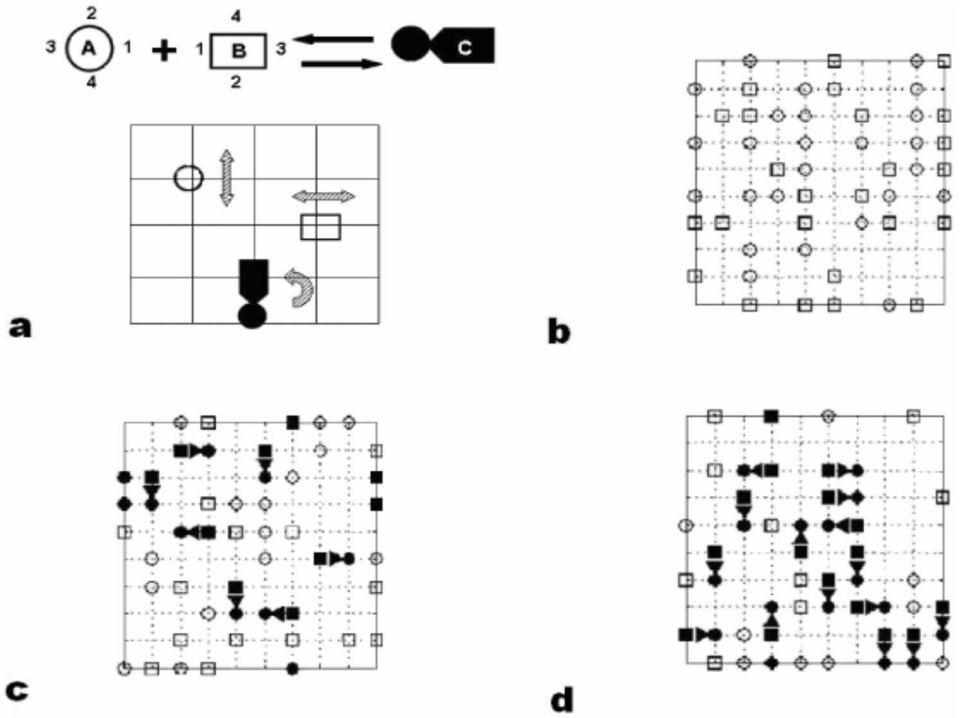


FIG. 1. Schematic of the lattice-based Monte Carlo model. (a) Illustration of the binding model. Two particles, *A* and *B*, must be adjacent on the lattice and present compatible binding sites (side 1) to one another to allow binding to form the complex *C*. (b) Initial configuration for a simulation with only *A* and *B* particles present. (c) *A* and *B* particles begin moving and rotating on the lattice according to a Brownian motion model. They meet and begin to form *C* dimers. (d) A steady state solution is reached when their average concentrations remain constant.

species than for smaller ones. Smaller molecules can more easily pass between obstacles and so the volume available to them is essentially the total unoccupied volume of the system. But for larger molecules the space between objects may not be sufficient to pass through and this volume becomes unavailable, or excluded, even though it is unoccupied. Crowding agents have been used experimentally to mimic background molecules. Typically these are inert particles that move throughout the solution by passive diffusion. However, this use of diffusing crowding agents may not be an appropriate model when considering the crowding effects produced by essentially stationary obstacles, such as intracellular compartments, cytoskeleton networks, and other large complexes. Here, we examine the effect of moving versus stationary obstacles on the association rate constants for heterodimer formations. We accomplish this through two-dimensional, lattice-based, Monte Carlo simulations. Simulations provide an especially robust framework for this application since the spatial environment can be incorporated directly into the model and discrete interactions can be observed and tracked and our Monte Carlo model can capture the inherently stochastic nature of molecular interactions. We examine these conditions, relevant to both *in vivo* and *in vitro* environments, and elucidate their differences.

## MODEL DESCRIPTION

We utilize a variation of a Monte Carlo model called LaBB (lattice based biological) Monte Carlo, developed previously to simulate molecular assembly of biopolymers in a crowded environment [22,23]. Binding in this model is based on the spatiotemporal arrangement of particles on the lattice. Conformational changes associated with dimer binding [12], but more related to molecular structure, are not implemented in this model. As seen in Fig. 1(a), two different types of monomers, *A* and *B*, must be located immediately adjacent to one another on the lattice with their binding sites correctly aligned for a heterodimer, *C*, to form. *C* can unbind into its constituent *A* and *B* parts. Dimers' and monomers' abilities to move and rotate about the lattice are dependent on a prescribed diffusion coefficient and the occupancy of the surrounding sites. The diffusion coefficient determines the percentage of particles that will be given a chance to move in a single iteration, provided their movement is not impeded by an adjacent particle. As shown in Figs. 1(b)–1(d), the solution progresses from initial conditions where *A* and *B* monomers are placed randomly on a lattice, to a condition where *C* dimers are being formed, and finally to an equilibrium condition where the molecular distributions are relatively stationary over time.

We can evaluate the quantitative impact of different crowding models on the reaction progress by measuring the effects of each model on the effective rate constants of the system. The method for extracting these from the Monte Carlo model is derived from the chemical rate equations for the continuum model of the process in the absence of crowding effects. Using the law of mass action, the process is described by the following systems of ordinary differential equations (ODEs):

$$\frac{d[A]}{dt} = -[A][B]k^{+} + [C]k^{-},$$

$$\frac{d[B]}{dt} = -[A][B]k^{+} + [C]k^{-},$$

$$\frac{d[C]}{dt} = [A][B]k^+ - [C]k^-. \quad (1)$$

Here $k^+$ is the binding rate constant and $k^-$ is the unbinding rate constant which are typically determined experimentally. The square brackets denote the total concentration of molecules of that particular type. The ODE model gives a continuous, deterministic solution of average behavior for a large, spatially uniform distribution of particles. It cannot, though, account for inhomogeneous conditions or discrete interactions. By numerical differentiation of Eq. (1) and considering binding and unbinding events as uncoupled, estimates for the rate constants can be obtained from the distribution of a single species over time,

$$k^+ = \frac{[A(t)] - [A(t+\Delta t)]}{[A][B]\Delta t},$$

$$k^- = \frac{[A(t\prime + \Delta t)] - [A(t\prime)]}{[C]\Delta t}. \quad (2)$$

Equation (2) can also be derived from a stochastic formulation of the chemical reaction [24] where $k^+\Delta t$ is defined as the average probability for a particular pair of $A$ and $B$ molecules to bind, $k^-\Delta t$ is the average probability for a particular dimer to unbind, and the quantity of molecules are expressed as integer numbers rather than concentrations. Considering $\Delta t$ as one iteration in the model, $k^-$ and $k^+$ are synonymous with the binding and unbinding probability, respectively.

Using Eq. (2) and the Monte Carlo model to track molecules over the course of a simulation, we can calculate the average rates for a single reaction trajectory and derive rate constants from the average of many trajectories. We can then compare the Monte Carlo model under different assumptions about crowding agents with the classical ODE model to study how crowding influences molecular assembly.

In the lattice model, the $k^+$ value is not explicit as implied by Eq. (1) but rather is a function of spatial conditions on the lattice. It is the product of two probabilities; that $A$ and $B$ monomers are adjacent to one another and that their binding sites are correctly oriented. Each monomer is considered to be four sided, one of which is a binding site. Therefore the probability that two monomers' binding sites are correctly aligned has a constant value of 1/16th. Any changes in the $k^+$ values obtained with the model can then be attributed to the influence of crowding on the relative positions of $A$ and $B$ monomers on the lattice. Crowding is assumed here to have little influence on unbinding events and so $k^-$ is specified explicitly in the model and is independent of the arrangement of particles on the lattice.

We first compare the Monte Carlo and ODE models at low concentrations of molecules, without inert particles, where spatial conditions are expected to have little effect on equilibrium conditions. This validates the Monte Carlo model and also provides a baseline for the other cases. We then consider three scenarios that have relevance in cellular environments but may deviate from the assumptions made by the ODE model. In the first scenario, the initial concentration of $A$ and $B$ monomers is progressively increased. This represents situations in which large numbers of reacting species localize in the cell to accomplish specific functions, such as is seen during cytokenesis and mitosis. In the second scenario, the concentration of $A$ and $B$ monomers are maintained constant while stationary inert particles are added and progressively increased. This mimics the nonspecific crowding effects of stationary structures found *in vivo* that do not actively participate in the reaction process, such as intracellular compartments, cytoskeleton networks or immobilized proteins. The third scenario is analogous to the second except the inert particles are permitted to move, imitating the nonspecific crowding effects of background molecules present in the cytosol that diffuse along with the reacting species but are not directly involved in the reaction process.

## RESULTS

We performed a series of simulations of the crowding models discussed above, varying the concentrations and estimating the rate constants for each. The model tracks discrete molecules and so the units of forward rates are per monomer per time step and of backward rates are per time step. These constants were then applied to the ODE model with the same initial concentrations and Eqs. (1) were numerically integrated to provide a comparison to a continuum model with the same effective rates. Unless otherwise noted, any Monte Carlo data presented are the mean from five simulations performed for 20 000 iterations each on a 100 $\times$ 100 lattice with periodic boundary condition. The reverse rate was fixed to 0.01 in all simulations. Using Eq. (2), the $k^-$ values were derived from the model for all cases discussed here and were consistently found to be 0.01, within a standard deviation three orders of magnitude lower than the reverse rate. We therefore do not discuss the reverse rates further below.

To compare the Monte Carlo model and the ODE model, we first ran a baseline Monte Carlo simulation of 500 $A$ and $B$ particles until equilibrium and calculated the rate constants as described above. The mean $k^+$ value derived from the Monte Carlo model was $2.55 \times 10^{-5}$. For comparison, we then varied concentrations of $A$ and $B$ monomers concurrently and independently. Figure 2 shows the results for two different initial conditions. Figures 2(a) and 2(b) compare results for 250 $A$ and $B$ monomers each at the initial time step. Figures 2(c) and 2(d) are the results using 100 $A$ monomers and 400 $B$ monomers. As can be observed in Fig. 2, the inferred rate constants are invariant across starting conditions at these low concentrations. Several combinations of diffusion rates were tested, yielding the same results at steady state. For the cases shown here all of the $A$ particles are given a chance to move every iteration while only one-half of the $B$ particles and one-fourth of the $C$ particles are given the chance.

To examine the effect of the species concentrations on dimer formation, the initial total number of $A$ and $B$ monomers was progressively increased from 100 to 7000, with equal amounts of $A$ and $B$ monomers used in each simulation. Figure 3 plots the inferred forward rate constants as a function of concentration for these experiments. This experi-

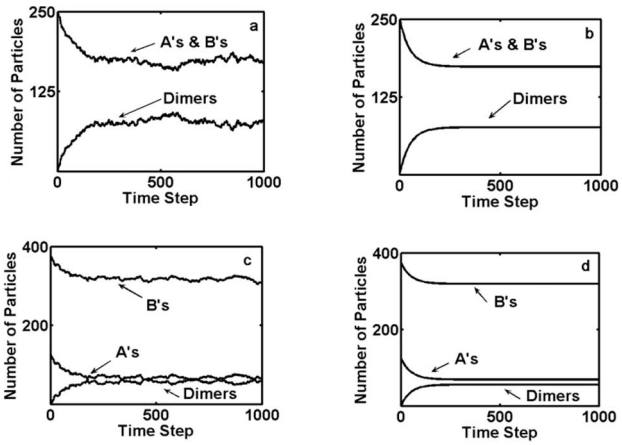


FIG. 2. Time history comparison of (a) Monte Carlo results for 250 *A* and 250 *B* monomers and (b) ODE results using the rate constants derived from the simulation of part (a). (c) Monte Carlo results for 100 A and 400 B monomers and (d) ODE results using the rate constants derived from the simulation of part (c).

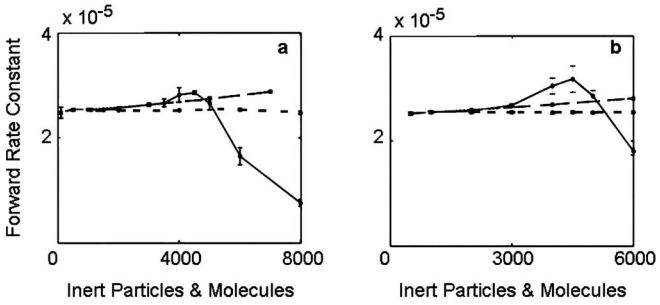


FIG. 3. The effects of crowding on binding rates for *A* and *B* molecules are shown for three cases; no inert particles (large dashed line); stationary inert particles (solid line); and moving inert particles (small dashed line); (a) model with differing diffusion rates between species (1 for *A*, 0.5 for *B*, 0.25 for *C*, 0.25 for inert). Increasing *A* and *B* molecules cause the binding rate to increase. Adding stationary inert particles has a bimodal effect and moving inert particles has little effect on binding rates. (b) Model with a single diffusion rate of 1 for all species. Experimental conditions are otherwise the same as in part (a).

ment and the others in this section were run in two variants: one giving a distinct diffusion rate to each species [Fig. 3(a)] and the other using the same diffusion rate for all diffusing species [Fig. 3(b)]. Up to 2000 monomers, the rate remains approximately constant in either variant. The rate then increases approximately linearly with increasing initial monomer concentration [large dashed line, Fig. 3(a)]. At 7000 initial monomers, the effective forward rate is 14% higher than that observed in low-concentration conditions.

We next examined the effect of stationary obstacles on molecular assembly by using a constant initial concentration of 1000 monomers (500 *A* and 500 *B*) with the same diffusion coefficients as previously stated while increasing the number of inert particles incrementally from 0 to 7000. Inert particles were positioned randomly on the grid at the beginning of each simulation and remained in this initial configuration throughout. Up to 2500 inert particles, or 3500 initial particles, counting the *A* and *B* monomers, the rates closely track those seen when increasing reactant monomer concentration. Between 3500 and 4500 initial particles, the rate increase is more pronounced than that produced with higher concentrations of reactant particles only. Beyond 4500 initial particles, there is a steep decline in the rate curve [solid line, Fig. 3(a)].

We finally allowed the inert particles to diffuse and again varied inert particle concentration for fixed reactant concentrations. The same conditions as the stationary case were maintained except that the inert particles were allowed to move with a diffusion coefficient equal to that of the dimers. Under these conditions, the inferred binding rate remains nearly constant over the entire range of inert particle concentrations [small dashed line, Fig. 3(a)].

## DISCUSSION

If only one *A* and one *B* particle were randomly placed on a lattice of *n* points, the probability, *p*, for them to be located next to one another with their binding sites correctly aligned is

$$p = k^{+}\Delta t = \frac{1}{4(n-1)}.$$

This probability gives the expected binding rate in a dilute, well-mixed environment. With $\Delta t$ equal to 1 and *n* equal to 10 000, $k^{+}$ is $2.5\times10^{-5}$, which is very close to the value obtained with the model ($2.55\times10^{-5}$) at total particle counts of below approximately 1000. This approximation however provides a generally poor model of the rates produced in crowded conditions. Although how the model fails depends on the exact assumptions of the crowding model.

Increasing numbers of reactant *A* and *B* particles tends to lead to increased binding rate (large dashed lines in Fig. 3). To explain this, in a crowded environment we can reasonably assume particles remain next to one another for longer periods of time, allowing adjacent *A* and *B* particles more opportunity to bind. Similarly dimers that unbind are more likely to rebind. Excluded volume effects cause the reaction to proceed as if the concentration of the solution were increasing superlinearly with solvent count because additional particles both add to the monomer count and displace otherwise free solution volume. The overall effect is to increase the probability to stay and is likely the cause for the increases seen here. A closer look at the binding rate curves shows that the slope is also increasing with increasing number of particles. We would expect excluded volume effects to become proportionately more pronounced as less free volume is available. Both results are consistent with previous predictions of the effect of crowding on heteroassociations [1].

In the next case, the number of the *A* and *B* monomers is maintained constant at a relatively low concentration of 500 each and increasing numbers of stationary inert particles are added incrementally. This case interestingly exhibits a bimodal behavior (solid lines in Fig. 3), as predicted by Minton

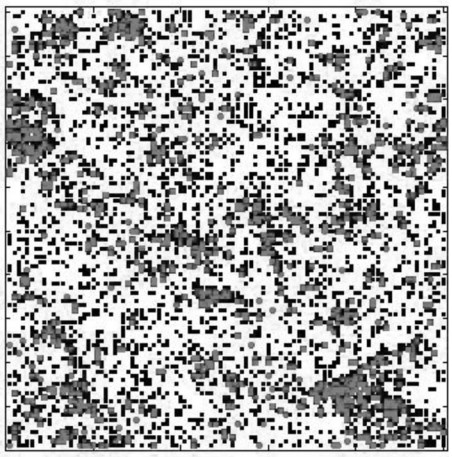

FIG. 4. The final time step from a realization with 4000 total particles; 3000 inert stationary particles (black squares), and 1000 moving reacting particles (gray circles and squares). The moving particles become trapped in regions where the partitioning of the stationary inert particles make it difficult to escape. The effect is compounded as more reacting particles become entrapped causing a sharp increase in the reaction rate.

[25]. Initially the rate increase is consistent with the previous case. Here again we suggest the increase in the reaction rate is caused by an excluded volume effect increasing the probability of reactant monomers to linger near one another. The effect now proceeds not due to high numbers of reacting particles but rather obstacles introduced by inert particles. With the number of pathways available for molecular diffusion reduced, traffic jams occur in the vicinity of the remaining particles, increasing the probability to stay. At 3000 particles the rate curve deviates from the previous case as the slope becomes more severe. At its peak the reaction rates exceed those seen when the entire population was a reacting species. We hypothesize that this secondary effect proceeds from inert particles creating more complicated structures that reactants have greater difficulty escaping. Trapping particles into subregions, many of which by chance have extremely high local concentrations would cause an additional increase in the rate constant beyond that expected from a simpler conception of excluded volume effects. Figure 4 illustrates this phenomenon. As more inert particles are added, beyond 4500 initial particles in Fig. 3(a) and 5000 in Fig. 3(b), the number of subregions increases as the local grid size decreases such that many reactants become completely isolated from one another. At extremely high concentrations, diffusion becomes impossible and the reaction rate constant necessarily falls.

Crowding agents produce very different effects when they are free to diffuse (small dashed lines in Fig. 3). Even at very high concentrations, no significant change in the reaction rate constant is seen. Monomers, dimers, and inert particles move at each iteration so that inert particles do not remain in one location long enough for traffic jams or isolated regions to form. In other words a well mixed, relatively homogeneous environment is maintained independent of inert particle concentrations. The binding rate thus remains constant at the level seen for the other cases at low concentrations. While the inert particles are likely to produce both excluded volume and impeded diffusion effects, the two effects would approximately cancel out under these conditions.

The results are qualitatively similar whether constant or variant diffusion rates were assumed for the different species, but some variations bear noting. For scenarios 1 and 3, the binding rates appear unaffected by the change in diffusion coefficients. For stationary inert particles though, the nonlinear behavior starts with slightly fewer inert particles and the maximum binding rate achieved is higher. The standard deviations between simulations are relatively large in these regions, though, and the differences between the diffusion models may therefore reflect random chance. These high deviations under conditions of high crowding likely reflect the importance of the spatial arrangement of the obstacles under high crowding conditions.

Our model does not explicitly consider conformational switching of subunits as part of the binding process and the results might be somewhat different for systems, such as Cdc42/CBD [12], in which substantial conformational change is coupled to binding. We would expect such systems to be relatively insensitive to the inhibitory effects of crowding but still sensitive to its excitatory effects, and therefore to have a comparatively greater rate increase in crowded conditions than is observed in our model. The coupling of binding and conformational switching was suggested by Caspar [26] to be a general mechanism for driving assembly reactions, which may explain the empirical observation that crowding, tends to drive assembly reactions even though simulation and first principles suggest crowding might inhibit them [1].

## CONCLUSION

The effect of the concentrations of reacting species on assembly processes is well recognized in theory but often neglected in *in vitro* experiments and computer models. The use of a lattice Monte Carlo model allows us to explore the importance of some model assumptions to the quantitative effects of crowding on biochemistry. Crowding influences reaction rates through several distinct mechanisms. Variations in assumptions about the nature of the crowding agent allow us to uncouple some of these effects and understand their individual impacts. The models tested here each correspond with sources of crowding expected *in vivo*. We find that the copy number of reacting species and the arrangement of intracellular structures both play important roles in the kinetics of assembly processes while background molecules have little influence. For moving inert particles, the correlation between the concentration of crowding agents and binding rates found with the model may seem contrary to experimental evidence that supports increasing reaction rates with increasing inert particle concentration [27,28]. In these cases, though, the crowding agents and/or the reacting species were polymers which likely exhibit greatly inhibited diffusion relative to the independent particles modeled here. No experimental data comparing stationary versus moving inert

particles over a range of concentrations could be found to validate or dispute the behavior observed in our simulations under those conditions. However it is consistent with the behavior observed in DNA kinase activity when high molecular weight polymers versus lower molecular weight crowding agents were added [10]. Our results underscore the difficulty of developing realistic models of crowding in the highly heterogeneous environment of the living cell [4].


[1] A. Minton, J. Biol. Chem. **276**, 10577 (2001).
[2] A. Arkin and H. H. McAdams, Genetics **149**, 1633 (1998).
[3] A. Baroffio and M. Bolt, J. Cell. Sci. **103**, 581 (1992).
[4] J. Peccoud and C. Jacob, Biophys. J. **71**, 101 (1996).
[5] F. Lanni, A. S. Waggoner, and D. L. Talor, J. Cell Biol. **100**, 1091 (1985).
[6] S. Cayley, B. A. Lewis, H. J. Guttman, and M. T. Record, Jr., Mol. Biol. **222**, 281 (1991).
[7] J. R. Ellis, Trends Biochem. Sci. **26**, 597 (2001).
[8] A. B. Fulton, Cell **30**, 345 (1982)
[9] A. G. Ogston and C. F. Phelps, Biochem. J. **78**, 827 (1960).
[10] S. B. Zimmerman and A. Minton, Annu. Rev. Biophys. Biomol. Struct. **22**, 27 (1993).
[11] A. Minton, Mol. Cell. Biochem. **55**, 119 (1983).
[12] Q. Lu, H. P. Lu, and J. Wang, Phys. Rev. Lett. **98**, 128105 (2007).
[13] B. Harrison and S. B. Zimmerman, Nucleic Acids Res. **14**, 1863 (1986).
[14] R. A. Lindner and G. B. Ralson, Biophys. Chem. **66**, 57 (1997).
[15] G. Rivas, J. A. Fernandez, and A. Minton, Biochemistry **38**(29), 9379 (1999).
[16] K. Snoussi and B. Halle, Biophys. J. **88**, 2855 (2005).
[17] S. Schnell and T. E. Turner, Prog. Biophys. Mol. Biol. **85**, 235 (2004).
[18] A. R. Kinjo and S. Takada, Phys. Rev. E **66**, 031911 (2002).
[19] H. Berry, Biophys. J. **83**, 1891 (2002).
[20] A. Minton, Biophys. J. **63**, 1090 (1992).
[21] A. Minton, Biophys. J. **55**, 805 (1989).
[22] K. Puskar, S. Ta'asan, R. Schwartz, and P. R. LeDuc, Mech. Chem. Biosyst. **1**, 123 (2004).
[23] K. Puskar, S. Ta'asan, R. Schwartz, and P. R. LeDuc, Cell Biochem. Biophys. **45**, 195 (2006).
[24] D. T. Gillespie, J. Phys. Chem. **81**, 2340 (1977).
[25] A. P. Minton, Int. J. Biochem. **22**, 1063 (1990).
[26] D. L. D. Caspar, Biophys. J. **32**, 103 (1980).
[27] D. Drenckhahn and T. D. Pollard, J. Biol. Chem. **261**, 12754 (1986).
[28] J. R. Wenner and V. A. Bloomfield, Biophys. J. **77**(6), 3234 (1999).